Liquid Phase Behavior of Ionic Liquids with Alcohols: Experimental Studies and Modeling

Jacob M. Crosthwaite, Mark J. Muldoon, Sudhir N. V. K. Aki, Edward J. Maginn, and Joan F. Brennecke*

Department of Chemical and Biomolecular Engineering, University of Notre Dame, Notre Dame, Indiana 46556

Received: January 11, 2006; In Final Form: March 11, 2006

Ionic liquids (ILs) have been suggested as potential "green" solvents to replace volatile organic solvents in reaction and separation processes due to their negligible vapor pressure. To develop ILs for these applications, it is important to gain a fundamental understanding of the factors that control the phase behavior of ionic liquids with other liquids. In this work, we continue our study of the effect of chemical and structural factors on the phase behavior of ionic liquids with alcohols, focusing on pyridinium ILs for comparison to imidazolium ILs from our previous studies. The impact of different alcohol and IL characteristics, including alcohol chain length, cation alkyl chain length, anion, different substituent groups on the pyridinium cation, and type of cation (pyridinium vs imidazolium) will be discussed. In general, the same type of behavior is observed for pyridinium and imidazolium ILs, with all systems studied exhibiting upper critical solution temperature behavior. The impacts of alcohol chain length, cation chain length, and anion, are the same for pyridinium ILs as those observed previously for imidazolium ILs. However, the effect of cation type on the phase behavior is dependent on the strength of the cation−anion interaction. Additionally, all systems from this study and our previous work for imidazolium ILs were modeled using the nonrandom two-liquid (NRTL) equation using two different approaches for determining the adjustable parameters. For all systems, the NRTL equation with binary interaction parameters with a linear temperature dependence provided a good fit of the experimental data.

Introduction

Ionic liquids (ILs) is the term used to describe a relatively new class of ionic compounds that are liquid at temperatures below 100 °C. Typically composed of organic cations with either organic or inorganic anions, ILs have negligible vapor pressure and a wide liquidus range, in excess of 300 K for many ionic liquids. Another interesting aspect of ILs is that the physical and chemical properties are dependent on the cation (including substituent groups on the cation) and anion. For example, changes in the cation and anion have been shown to have a large impact on properties such as gas and liquid solubilities, density, melting point, glass transition temperature, and viscosity.[1−4] With detailed knowledge of the impact of different characteristics of ILs on the physical and chemical properties, it should be possible to develop "designer" ILs with properties for use in specific applications, such as liquid−liquid extraction or reactions, by the choice of the cation and anion of the IL.

This work is a continuation of our previous studies,[2,5] which focused on the liquid−liquid-phase equilibrium of imidazolium ionic liquids. In this study, we investigated the liquid−liquid-phase equilibrium of pyridinium ionic liquids with alcohols. Characteristics investigated here include the effect of alcohol chain length (1-butanol vs 1-hexanol), cation alkyl chain length (butyl vs hexyl), anion (BF_4 vs $(CF_3SO_2)_2N$ (bis(trifluoromethylsulfonyl)imide or Tf_2N)), and different substituent groups on the cation (methyl, dimethylamino). A comparison of the phase behavior for analogous pyridinium and imidazolium ILs is discussed. In addition to experimental work, all IL/alcohol systems are modeled using the general nonrandom two-liquid (NRTL) equation using two different approaches for determining the adjustable binary interaction parameters: (1) temperature-independent parameters and (2) linear temperature-dependent parameters. A comparison of these two approaches is presented, along with adjustable parameters for all systems investigated in this work and our previous studies.

Experimental Section

Materials. The list of alcohols used in this study, including CAS number, source and grade, and water content (determined by Karl Fisher titration, EM Science Aquastar V-200 Titrator) is as follows: 1-propanol (71-23-8, Aldrich 99.5% anhydrous, 860 ppm water), 1-butanol (71-36-3, Aldrich 99.8% anhydrous, 250 ppm water), 1-hexanol (111-27-3, Aldrich 99+% anhydrous, 590 ppm water). All alcohols were used without further purification.

A list of all the cations and anions used in this study, along with their structures and abbreviations, is shown in Table 1. All ILs except [bmpy][Tf_2N] were synthesized in our laboratory using standard procedures.[6,7] Typical synthesis and purification procedures have been published in our previous work.[2,3,5] Impurity levels of halide (Br^-) and ammonium ions (for [bmpy][BF_4] only) for the ILs synthesized in-house were measured using an Oakton Ion 510 meter with Cole-Parmer Ion Specific Probes (27502-05 for Br^- and 27502-03 for NH_4^+). All values were less than 10 ppm for Br^- and less than 20 ppm for NH_4^+. [bmpy][Tf_2N] was obtained from Strem Chemicals with a purity of ≥99% and was used as received. All ILs were dried under vacuum for at least 48 h at temperatures between 313 and 353 K before use to remove organic solvents and water, and the water content was determined by Karl Fisher titration. The water content for all ILs used in this study is as follows: [bmpy][BF_4], 320 ppm; [bmpy][Tf_2N], 160 ppm; [hpy][Tf_2N], 100 ppm;

10.1021/jp060201a CCC: $33.50
Published on Web 04/14/2006

TABLE 1: List of Cations and Anions Investigated

Formal Name	Structure	Abbreviation
1-n-butyl-3-methylpyridinium	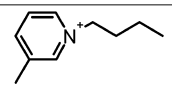	[bmpy]
1-n-hexylpyridinium	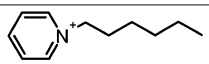	[hpy]
1-n-hexyl-3-methylpyridinium	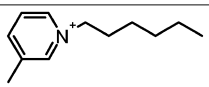	[hmpy]
1-n-hexyl-3,5-dimethylpyridinium	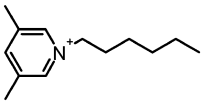	[hmmpy]
1-n-hexyl-3-methyl-4-dimethylaminopyridinium	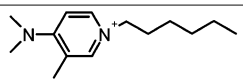	[hmDMApy]
1-n-hexyl-2-ethyl-3,5-dimethylpyridinium	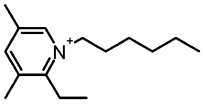	[hemmpy]
Tetrafluoroborate		[BF_4]
Bis(trifluoromethylsulfonyl)imide	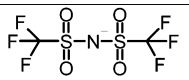	[Tf_2N]

[hmpy][Tf_2N], 190 ppm; [hmmpy][Tf_2N], 100 ppm; [hmDMApy]-[Tf_2N], 410 ppm; [hemmpy][Tf_2N], 150 ppm.

Experimental Method. All experiments to determine the liquid−liquid equilibria (LLE) of the ionic liquid-alcohol systems were conducted using a "cloud-point" method, similar to that described by Marsh[8] and used in our previous studies.[2,5] In this technique, a sample of known composition was placed in a viewcell and heated until it was one phase. The "cloud point temperature" is the temperature at which the sample initially changes from one phase to two phases. The phase transition is observed visually. In our apparatus, four ionic liquid−alcohol solutions of different concentrations were prepared gravimetrically in 5 mL viewcells in a glovebox, sealed from the atmosphere, and placed in a water bath. The uncertainty in the compositions is estimated to be ±0.0001 mole fraction. The samples were heated in the water bath using a 1000 W immersion heater to about 5 K above the highest expected cloud point temperature and maintained at that temperature for 10 min. The samples were cooled using a recirculating water chiller at a cooling rate of about 1 K/min. The temperature of each sample was individually measured using a T-type thermocouple immersed in the sample. The experiment was repeated four additional times to determine accurate and reproducible values (±0.5 K). The reproducibility of the cloud point temperatures for replicate samples of the same composition and for different batches of ionic liquid and alcohol is within ±0.5 K.

Results and Discussion

For this study, the liquid-phase behavior for a number of binary ionic liquid−alcohol systems was determined. As mentioned above, Table 1 shows all anions and cations used in this study, including structure, formal name, and abbreviation. The systems investigated are shown below and are broken down by ionic liquid:

[bmpy][BF_4]: 1-propanol, 1-butanol

[bmpy][Tf_2N]: 1-butanol, 1-hexanol

[hpy][Tf_2N]: 1-hexanol

[hmpy][Tf_2N]: 1-hexanol

[hmmpy][Tf_2N]: 1-hexanol

[hmDMApy][Tf_2N]: 1-hexanol

[hemmpy][Tf_2N]: 1-hexanol

Results in the form of $T-x$ data for each binary system investigated are shown in the Supporting Information. Similar characteristics were observed for all of the liquid−liquid equilibrium systems examined. For example, upper critical solution temperature (UCST) behavior was observed in all systems. In addition, the alcohol-rich phase was observed to have a low concentration of ionic liquid of about 1−2 mol % IL, while the ionic liquid-rich phase was observed to have a large concentration of alcohol, sometimes in excess of 50 mol % alcohol. With the systems listed above, the impact on the phase behavior of different alcohol and ionic liquid factors was determined.

Alcohol Factors

Effect of Alcohol Chain Length. Figure 1 shows the liquid-phase behavior for the ionic liquid [bmpy][BF_4] with the alcohols 1-propanol and 1-butanol. From the figure, it is clear that the UCST increases as the chain length of the alcohol increases from approximately 306 K for 1-propanol to 322 K for 1-butanol. At a given temperature the change is most obvious for the IL-rich phase, since the alcohol concentration in that phase decreases substantially when the alkyl chain on the alcohol is lengthened. Since the IL solubility in either alcohol is quite small, changes in the composition of the alcohol-rich phase are not quite so obvious. Clearly, the mutual solubility of the IL and alcohol decrease with increasing alcohol chain length; the same trend is observed for [bmpy][Tf_2N] with 1-butanol and 1-hexanol in Figure 2. These observations are consistent with other ionic liquid systems reported in the literature, such as in our previous studies of imidazolium ILs with primary and secondary alcohols,[2,5] the study by Heintz et al. of [emim][Tf_2N] with a series of primary alcohols,[9] the study of [emim][PF_6] with a series of primary and secondary alcohols,[10] the study of solid−liquid equilibrium of [C_{12}mim][Cl] with a series of alcohols,[11] and the study of [BF_4] and [PF_6] ionic liquids with alcohols by Wagner et al.[12] By making the chain longer, the alcohol becomes more aliphatic and hydrophobic. *In all cases, the more hydrophobic the alcohol, the higher the UCST.*

Ionic Liquid Factors

Effect of Alkyl Chain Length on the Cation. Figure 3 shows the liquid-phase behavior for the ionic liquids [bmpy][Tf_2N] and [hmpy][Tf_2N] with 1-hexanol. As the alkyl chain length on the cation increases from a butyl group to a hexyl group, the UCST of the system decreases, from approximately 335 K for [bmpy][Tf_2N] to 310 K for [hmpy][Tf_2N]. The mutual solubility of both IL and alcohol increase at any particular temperature below the UCST with an increase in the cation alkyl chain length, with a larger increase in the alcohol solubility in the IL phase, compared to the IL solubility in the alcohol phase.

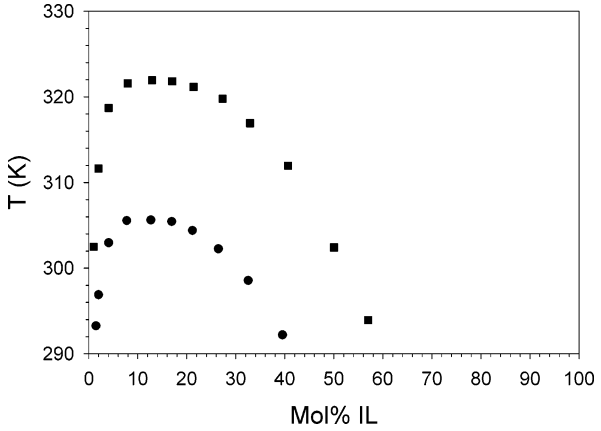

Figure 1. $T-x$ diagram for [bmpy][BF_4] with 1-propanol (●) and 1-butanol (■).

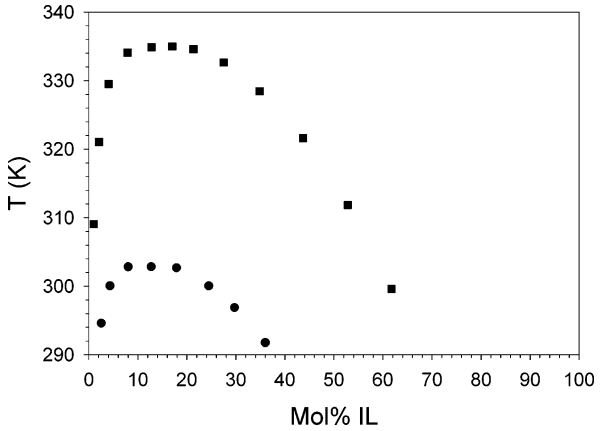

Figure 2. $T-x$ diagram for [bmpy][Tf_2N] with 1-butanol (●) and 1-hexanol (■).

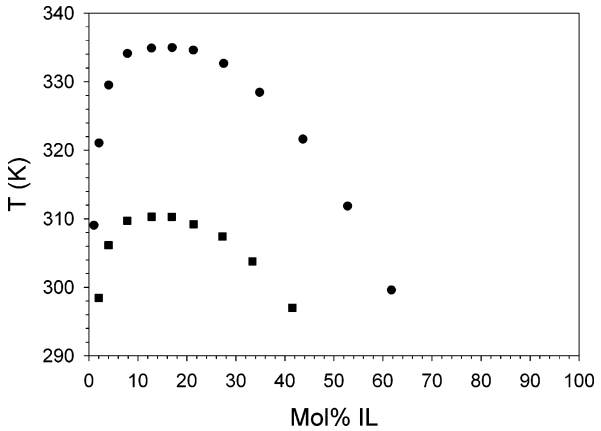

Figure 3. $T-x$ diagram for [bmpy][Tf_2N] (●) and [hmpy][Tf_2N] (■) with 1-hexanol.

From the literature, Wu et al. showed this trend clearly in their study of 1-alkyl-3-methylimidazolium [PF_6] ionic liquids (butyl, pentyl, hexyl, heptyl, and octyl) with 1-butanol,[8] as well as Wagner et al. in their study of [BF_4] and [PF_6] ionic liquids with alcohols (UCST values only)[12] and our previous studies of imidazolium ILs.[2,5] With increase of the chain length on the cation, the van der Waals (i.e., London dispersion forces) interactions increase between that chain and the alkyl portion of the alcohol. This increase in van der Waals interactions between alkyl portions of the cation and the alcohol is responsible for the enhancement in the mutual solubility of the IL and the alcohol and reduction in the UCST. The longer alkyl chain on the cation causes its "hydrophobicity" to more closely match

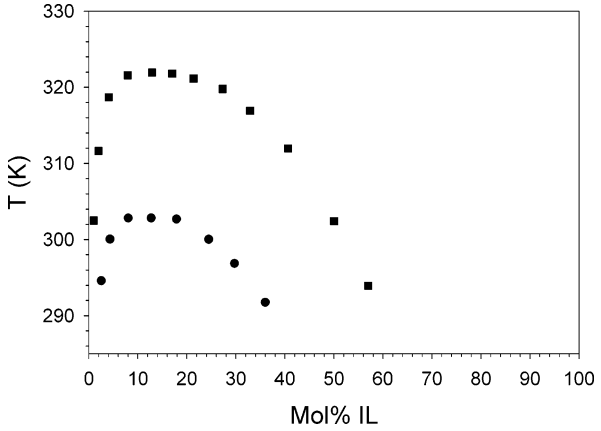

Figure 4. $T-x$ diagram for [bmpy][Tf_2N] (●) and [bmpy][BF_4] (■) with 1-butanol.

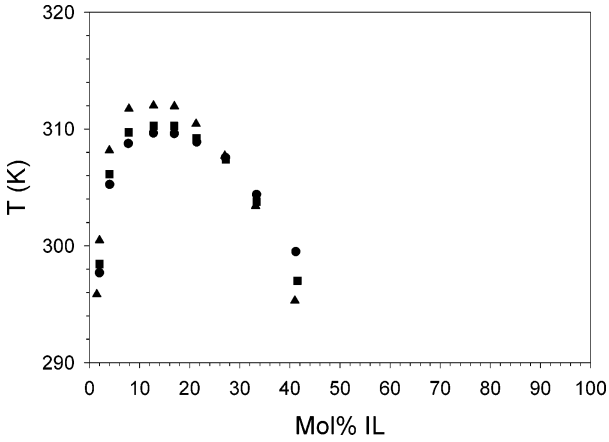

Figure 5. $T-x$ diagram for [hpy][Tf_2N] (●), [hmpy][Tf_2N] (■), and [hmmpy][Tf_2N] (▲) with 1-hexanol.

that of the alcohol. *Increasing the alkyl chain length on the cation of the IL lowers the UCST with alcohols, by increasing dispersion forces with their hydrophobic functionality*.

Anion. The influence of the anion can be examined by comparing the cloud point curves of several [bmpy] ionic liquids with a single alcohol. Figure 4 shows the liquid-phase behavior for [bmpy][Tf_2N] and [bmpy][BF_4] with 1-butanol. The UCST is lower for [bmpy][Tf_2N], at approximately 303 K. However, the UCST increases to over 322 K for [bmpy][BF_4]. Additionally, the phase envelope for the system increases greatly as the anion changes from [Tf_2N] to [BF_4], indicating that the mutual solubility of IL and alcohol at temperatures below the UCST decreases significantly as the anion of the IL is changed from [Tf_2N] to [BF_4]. This trend is consistent with our previous studies of imidazolium [Tf_2N] and [BF_4] ILs.[2,5] The higher UCST for [bmpy][BF_4] with butanol is likely due to strong anion/cation interactions that make the BF4 anion less available for hydrogen bonding with the butanol. With [bmpy][Tf_2N] the cation/anion interactions are weaker, allowing more hydrogen bonding between the butanol and the Tf_2N anion. Thus, the [bmpy][Tf_2N]/butanol system can have a lower UCST even if the strength of a Tf_2N/butanol interaction is less than the strength of a BF_4/butanol interaction. Thus, the choice of anion has a dramatic effect on the phase behavior of ionic liquids with alcohols. *Increasing the interaction between the anion and the alcohol lowers the UCST.*

Methyl Substitution. Figure 5 shows the liquid-phase behavior for [hpy][Tf_2N], with no methyl groups, [hmpy][Tf_2N], with one methyl group, and [hmmpy][Tf_2N], with two methyl groups, with 1-hexanol. The addition of a methyl group increases

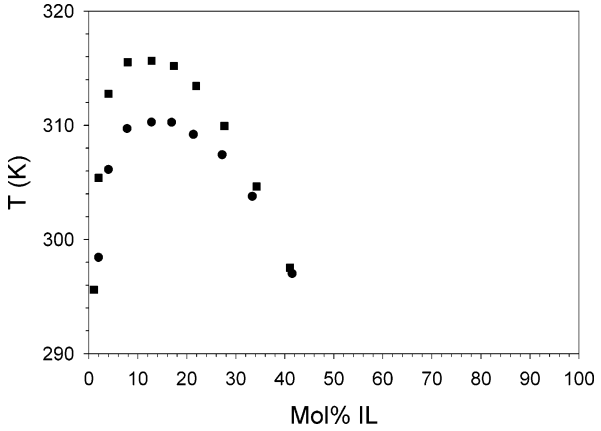

Figure 6. $T-x$ diagram for [hmpy][Tf_2N] (●) and [hmDMApy][Tf_2N] (■) with 1-hexanol.

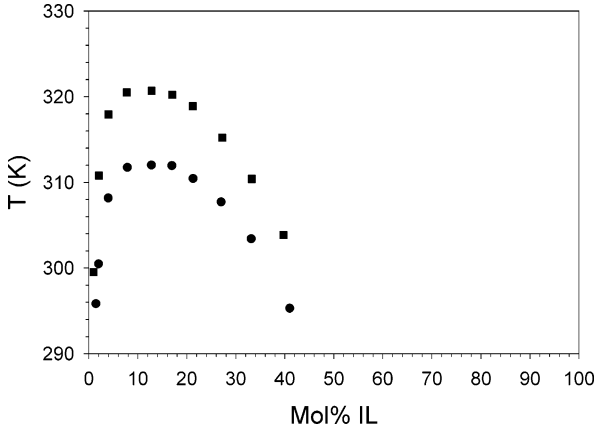

Figure 7. $T-x$ diagram for [hmmpy][Tf_2N] (●) and [hemmpy][Tf_2N] (■) with 1-hexanol.

the UCST slightly by about 1 K from 310 K for [hpy][Tf_2N] to 311 K for [hmpy][Tf_2N] and 312 K for [hmmpy][Tf_2N]. Starting with the alcohol-rich phase, the IL solubility in the alcohol decreases slightly as methyl groups are added to the cation. For example, the cloud point temperature, i.e., the temperature at which the sample transformed from one phase to two phases, for samples of 2 mol % IL (on the alcohol-rich side of the phase envelope), increases slightly as the number of methyl groups on the cation increases, from about 298 K for [hpy][Tf_2N] to 301 K for [hmmpy][Tf_2N]. From this observation, the decrease in IL solubility in the alcohol with increasing number of methyl groups can be inferred since the concentration of IL with the same cloud point temperature will be less for [hmmpy][Tf_2N] than for [hmpy][Tf_2N], which is less than that for [hpy][Tf_2N]. This trend remains until the cloud point curves intersect, at about 27 mol % IL, on the IL-rich side of the phase envelope. This crossover indicates that the alcohol solubility in the ionic liquid increases with increasing number of methyl groups on the cation. This evaluation can be inferred again by looking at the cloud point temperature for all three ILs at the same concentration, approximately 41 mol % IL. At this concentration, [hpy][Tf_2N], with no methyl groups, has the highest cloud point temperature at 299.5 K, while [hmmpy][Tf_2N], with two methyl groups, has the lowest cloud point temperature at 295.3 K. Therefore, with increasing number of methyl groups on the pyridinium cation, the IL solubility in the alcohol decreases slightly, while the alcohol solubility in the IL increases. This result, although based on very small changes in the cloud point temperatures, may be due to the increased size of the IL due to the addition of a methyl group. By addition of a methyl group to the cation, the free volume in the ionic liquid should increase to some extent, allowing more alcohol molecules to dissolve in the IL-rich phase. Conversely, the larger size of the cation with additional methyl groups will prevent more of the IL molecules from dissolving in the alcohol-rich phase. However, *the relative change in the phase behavior by the addition of methyl groups to a pyridinium cation is miniscule when compared to other characteristics of the IL, such as anion or cation alkyl chain length*.

Dimethylamino Group. The effect of adding a dimethylamino group (DMA) to a pyridinium IL is presented in Figure 6, which shows the cloud point curves for [hmpy][Tf_2N] and [hmDMApy][Tf_2N] with 1-hexanol. It was speculated that the addition of a DMA group at the 4 position of the pyridinium cation would have a significant impact on the cloud point curve since the DMA group should significantly change the electronic structure of the cation by more evenly distributing the positive charge about the ring. However, from Figure 6, the UCST increases only by about 5 K with the addition of the DMA group. In addition, it appears that the IL solubility in the alcohol decreases with the addition of the DMA group, while the alcohol solubility in the IL is either similar or possibly enhanced at lower temperatures with a DMA group. Although the change in the electronic structure of the cation with the presence of a dimethylamino group does have some effect on the phase behavior, its overall impact is not as significant as cation alkyl chain length or anion. *Addition of a substituent to the pyridinium ring that should significantly alter the charge distribution on the ring had very little effect on the phase behavior with alcohols*.

C2 Substitution. The effect of C2 substitution on a pyridinium cation was evaluated and is shown in Figure 7 for [hmmpy][Tf_2N] and [hemmpy][Tf_2N] with 1-hexanol. The only difference between these two compounds is an ethyl chain on the carbon adjacent to the nitrogen. From the figure, the UCST of the system increases by about 10 K and the mutual solubility of IL and alcohol decreases at temperatures below the UCST with the addition of an ethyl group at the C2 position. Similar behavior is observed for imidazolium ILs with the addition of a methyl group at the C2 position of the cation, although the increase in UCST is significantly larger with the imidazoliums, about 25 K.[5] The hydrogen at the C2 position is known to be very acidic for imidazolium cations,[13] and the increase in UCST due to the substitution of a methyl group at the C2 position for imidazolium cations has been attributed to a decrease in hydrogen bonding interactions between the alcohol and cation through the C2 hydrogen. However, ab initio studies have shown that while the hydrogens on a pyridinium cation do possess a small positive charge, the charges are very similar and are not as acidic as the C2 hydrogen of an imidazolium cation.[14] Therefore, the observed change in the phase behavior is probably not due to a significant decrease in hydrogen bonding between the cation through the C2 hydrogen and the alcohol, as with imidazolium cations. As mentioned earlier in this and previous studies, it has been shown that the alkyl portion of the alcohol interacts with the alkyl portion of the cation via van der Waals interactions. We speculate that the ethyl group at the C2 position of the pyridinium cation impedes the favorable alkyl−alkyl interaction between the long (hexyl) alkyl chain on the nitrogen and the alcohol, thus decreasing the mutual solubility of the IL and alcohol and increasing the UCST. *Substitution at the C2 position on a pyridinium cation has less of an impact on the phase behavior than for an imidazolium cation, presumably due*

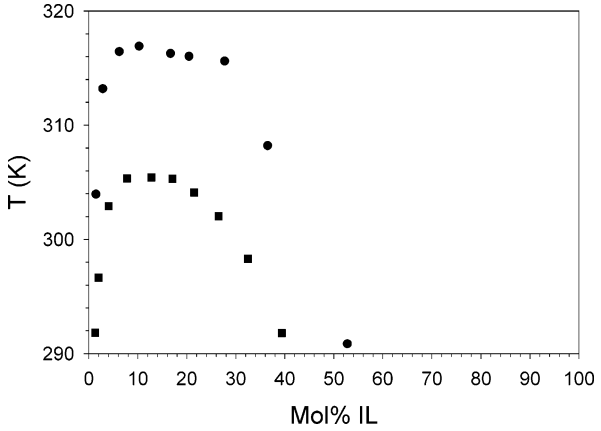

Figure 8. $T-x$ diagram for [bmim][BF_4][2] (●) and [bmpy][BF_4] (■) with 1-propanol.

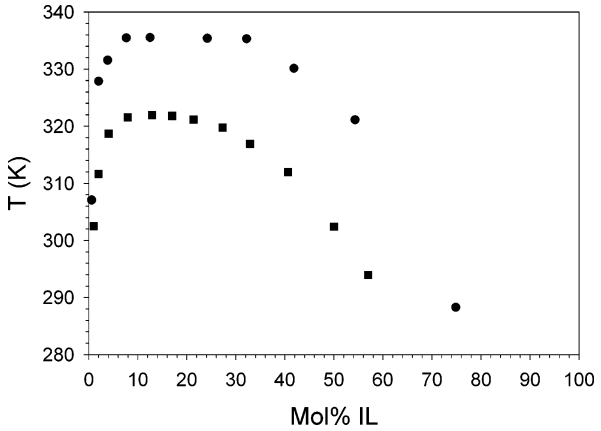

Figure 9. $T-x$ diagram for [bmim][BF_4][2] (●) and [bmpy][BF_4] (■) with 1-butanol.

to the type of interactions involved, van der Waals interactions, and steric hindrance versus hydrogen bonding.

Cation Type. A comparison of the phase behavior of pyridinum and imidazolium cations can be assessed by examining the phase curves for ionic liquids with the same anion and alcohol. Starting with the [BF_4] anion, Figure 8 shows the cloud point curves for [bmpy][BF_4] and [bmim][BF_4][2] with 1-propanol, while cloud point curves for the same ILs with 1-butanol are shown in Figure 9. In both figures, the UCST of the cloud point curve is higher for the imidazolium cation than the corresponding pyridinium cation by about 10 K, with lower mutual solubility of the IL and alcohol at temperatures below the UCST for the imidazolium cation. However, the opposite trend is observed for ionic liquids with the [Tf_2N] anion, as shown in Figure 10 for [bmpy][Tf_2N] and [bmim][Tf_2N][2] with 1-butanol, Figure 11 for the same ILs with 1-hexanol, and Figure 12 for [hmpy][Tf_2N] and [hmim][Tf_2N][5] with 1-hexanol. The UCST for the [Tf_2N] cloud point curves is higher for the pyridinium cations than the respective imidazolium cations by about 3−4 K, with a slightly lower mutual solubility of the IL and alcohol for the pyridinium cations. Moreover, there is evidence, from Figure 11, that the cloud point curves crossover at some temperature below the UCST, so that the alcohol solubility in the IL phase is higher for ILs with the pyridinium cation than the equivalent imidazolium cation. This observation leads to an interesting question as to why the effect of cation type is dependent on the anion of the ionic liquid.

Ab initio calculations suggest that the [BF_4] anion strongly associates with the imidazolium cation near the acidic hydrogen on the C2 carbon of the ring.[15] Although the [Tf_2N] anion does

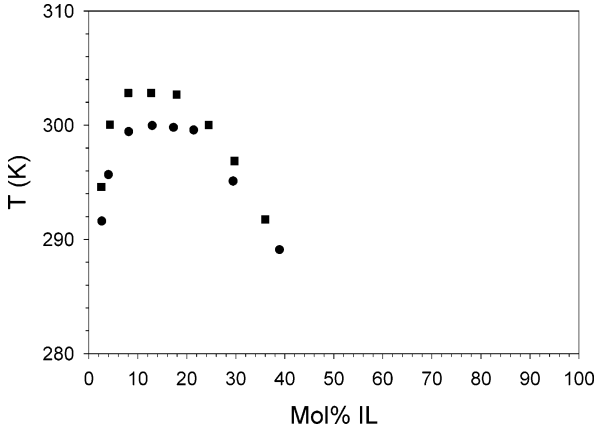

Figure 10. $T-x$ diagram for [bmim][Tf_2N][2] (●) and [bmpy][Tf_2N] (■) with 1-butanol.

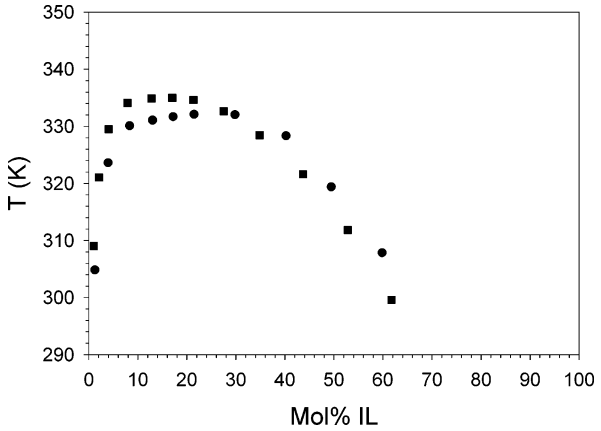

Figure 11. $T-x$ diagram for [bmim][Tf_2N][2] (●) and [bmpy][Tf_2N] (■) with 1-hexanol.

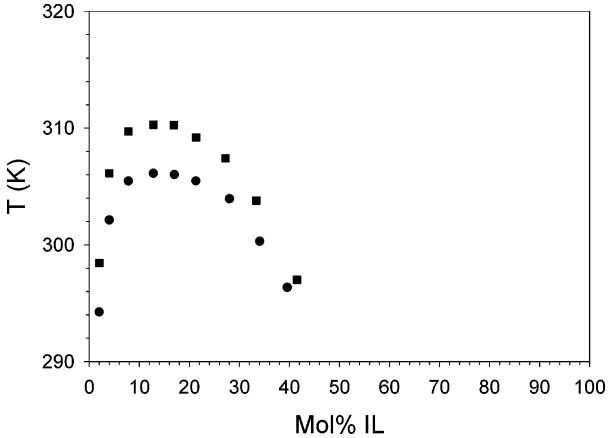

Figure 12. $T-x$ diagram for [hmim][Tf_2N][5] (●) and [hmpy][Tf_2N] (■) with 1-hexanol.

associate with the imidazolium cation at a similar position as the [BF_4] anion and can hydrogen bond to water and alcohols, [Tf_2N] coordinates more weakly to the imidazolium cation, as compared to [BF_4], most likely due to the significantly larger size of a [Tf_2N] anion and differences in the charge distribution for the two anions. However, as stated previously, the hydrogens on a pyridinium cation are not as acidic as the C2 hydrogen on a corresponding imidazolium cation, which means the [BF_4] anion will not associate as strongly with a pyridinium cation, compared to an imidazolium cation. By reduction of the interaction between the cation and anion, the alcohol in the mixture may be able to interact with both the cation and anion

to a larger degree. This increase in cation−alcohol and anion−alcohol interactions for [bmpy][BF_4] may account for the observed increase in the mutual solubility of the IL and alcohol and reduction of the UCST, compared to [bmim][BF_4].

Although the absence of a very acidic hydrogen on a pyridinium cation may reduce the overall cation−anion interaction for an IL with a [Tf_2N] anion, the difference in the strength of the cation−anion interaction of [Tf_2N] with an imidazolium versus a pyridinium cation is probably much smaller than that for a [BF_4] anion. Therefore, the strength of the cation−alcohol interactions will play a large role in the phase behavior. As stated previously, the hydrogens on a pyridinium cation do possess a small positive partial charge, but they are not as acidic as the C2 hydrogen on the imidazolium ring. This difference most likely accounts for the small difference in the UCST for imidazolium and pyridinium [Tf_2N] ionic liquids, with the cation−alcohol interactions of the imidazolium ILs slightly stronger than those for pyridinium ILs. Molecular dynamics simulations support the explanation of the trends of the UCSTs of [bmim][BF_4], [bmpy][BF_4], [bmim][Tf_2N], and [bmpy][Tf_2N] presented here.[14]

Additionally, the free volume of the IL may be larger for the pyridinium IL since a pyridinium cation is slightly larger than a corresponding imidazolium cation, allowing for the alcohol to dissolve to a greater degree in [bmpy][Tf_2N] than in [bmim]-[Tf_2N]. Greater free volume in [bmpy][Tf_2N] than in [bmim]-[Tf_2N] may account for the observed crossover of the IL-rich branches of the cloud point curves in Figure 11, with higher alcohol solubility in the IL-rich phase of the [bmpy][Tf_2N] system. Clearly, the strength of the cation−anion interaction, or the associating ability of the cation and anion, will be a major determining factor on the impact of the cation type on the liquid-phase behavior of IL/alcohol systems. *The relative strengths of cation/anion, cation/alcohol, anion/alcohol, and alcohol/alcohol interactions determines the liquid−liquid phase behavior of ionic liquids with alcohols*.

Modeling

In addition to cloud point curves, all IL/alcohol systems with liquid−liquid phase behavior were modeled using the nonrandom two-liquid (NRTL)[16] equation for a mixture of two components. The two components for the equation are (1) the IL, with the cation and anion as one overall species, and (2) the alcohol. The model assumes that the anion and cation remain completely associated, which may not be a good assumption for very dilute solutions of IL in alcohol. Nonetheless, we use this model to correlate the experimental data. Moreover, as will be shown below, the model parameters are an indication of relative strengths of interactions between the species in solution and reasonable values are obtained. The two parameters in the model are Δg_{12} and Δg_{21}. The first parameter, Δg_{12}, is the strength of the IL/alcohol interaction minus the strength of the alcohol/alcohol interaction. The second parameter, Δg_{21}, is the strength of the IL/alcohol interaction minus the strength of the IL/IL interaction.

Two different approaches were evaluated for determining the adjustable parameters of the NRTL equation, Δg_{12} and Δg_{21}, for each binary mixture. The first approach was to consider no temperature dependence for the adjustable parameters, i.e., the same parameters regardless of temperature for each binary. A double iterative method was employed for this work. We used the NRTL model for the activity coefficients of each component in each phase, γ_i, and solved the equifugacity condition required for phase equilibrium, shown by the equation

$$x_i^{\mathrm{I}}\gamma_i^{\mathrm{I}}(T, P, x_i^{\mathrm{I}}) = x_i^{\mathrm{II}}\gamma_i^{\mathrm{II}}(T, P, x_i^{\mathrm{II}}) \quad (1)$$

where the activity coefficients are evaluated at the temperature and pressure of the system and for the composition in each phase. Equation 1 is subject to the requirements that the mole fraction in each phase sum to unity

$$\sum x_i^{\mathrm{I}} = 1 \quad (2a)$$

$$\sum x_i^{\mathrm{II}} = 1 \quad (2b)$$

The two parameters of the NRTL model, Δg_{12} and Δg_{21}, were adjusted to minimize the sum of the square of the deviation, $\phi(x)$, between the experimental compositions (the set of x vs T data for each system) and those calculated from the NRTL model

$$\phi(x) = \sum^{i}\sum^{j}(x_{i,\mathrm{calc}}^{j} - x_{i,\mathrm{exp}}^{j})^2 \quad (3)$$

The SOLVER function in Microsoft EXCEL was used to adjust the parameters such that the objective function was minimized, providing the set of temperature-independent adjustable parameters for that particular binary system.

In the second approach, the adjustable parameters are allowed to have a linear temperature dependence, described by the equation

$$\Delta g_{ij} = a_{ij} + b_{ij}T \quad (4)$$

which follows observations by Renon and Prausnitz.[16] All calculations for this approach were made using a method based on interval analysis; this method will be described in detail elsewhere.[17] LLE data for the system in the form of composition data for both liquid phases for one of the species, x_1^{I} and x_1^{II}, at each temperature provides the input for the method. Note that in the cloud point method the compositions of the two liquid phases are never determined at exactly the same temperature. Therefore, these values were obtained from a smoothed curve through the experimental data. For each temperature, the equifugacity condition shown in eq 1 is solved for both species using interval analysis. Since there are two equations (equifugacity condition for each species) with two unknowns (adjustable parameters), exact values for Δg_{12} and Δg_{21} at each temperature are determined. This equation system may have multiple solutions, only one of which is physically realistic.[18] The use of interval analysis provides a guarantee that *all* the solutions are found, so that the physically most appropriate solution is not missed. The Δg_{12} and Δg_{21} values are then fit to the linear equation (eq 4) and the terms for the temperature-dependent adjustable parameters, a_{ij} and b_{ij}, are determined for each system, along with the corresponding uncertainty for each term. For each temperature investigated, the adjustable parameters from the linear fit (eq 4) are calculated, and then used to determine the calculated phase compositions by again solving the equifugacity condition (eq 1) with those adjustable parameters. Note that the data points right at the UCST were omitted from the fitting procedures since we would not expect an analytical mean field model like the NRTL equation to adequately capture behavior near a critical point. In fact, when attempted, we found that those points did not follow the linear temperature-dependent trend. The deviation, σ, for each IL/alcohol system was determined as the sum of the normalized

TABLE 2: Adjustable Parameters for All IL/Alcohol Systems Investigated with Two Liquid Phase Behavior

		Δg_{12} (J/mol)		Δg_{21} (J/mol)		
IL (1)	alcohol (2)	a	b	a	b	deviation, σ
[bmim][BF_4]	1-propanol	21100± 1500	−82 ± 4.9	33500 ± 2200	−61 ± 7.1	0.69
[bmim][BF_4]	1-butanol	19400 ± 2000	−69 ± 6.0	32200 ± 7100	−57 ± 21.9	0.80
[bmim][BF_4]	1-hexanol	24300 ± 4600	−75 ± 12.9	37900 ± 6600	−70± 18.4	0.84
[bmim][BF_4]	2-propanol	26700 ± 2100	−101 ± 6.7	27300 ± 4700	−38 ± 15.0	0.40
[bmim][BF_4]	2-butanol	33300 ± 2700	−116 ± 8.4	15300 ± 2200	1.4 ± 6.7	0.70
[bmim][BF_4]	isobutanol	23700 ± 1300	−85 ± 3.9	50500 ± 5800	−108 ± 17.5	0.88
[bmim][BF_4]	*tert*-butanol	28600 ± 1400	−106 ± 4.3	5600 ± 3100	35 ± 9.7	0.19
[hmim][BF_4]	1-butanol	24900 ± 1600	−98 ± 5.1	46900 ± 3700	−105 ± 12.0	0.25
[hmim][BF_4]	1-hexanol	23500 ± 1200	−85 ± 3.7	28500 ± 2600	−43 ± 8.1	0.22
[hmim][BF_4]	1-octanol	30700 ± 2600	−101 ± 7.5	43900 ± 2300	−88 ± 6.8	0.97
[omim][BF_4]	1-hexanol	38800 ± 1300	−147 ± 4.2	29000 ± 7200	−47 ± 24.1	0.19
[omim][BF_4]	1-octanol	29500 ± 3700	−110 ± 11.9	47000 ± 7100	−103 ± 23.0	0.48
[bmpy][BF_4]	1-propanol	21900 ± 1000	−88 ± 3.4	24300 ± 200	−34 ± 0.6	0.13
[bmpy][BF_4]	1-butanol	26800 ± 2000	−98 ± 6.5	24000 ± 800	−31 ± 2.6	0.64
[pmmim][Tf_2N]	1-butanol	19700 ± 2100	−73 ± 6.5	19600 ± 2900	−17 ± 8.9	0.23
[pmmim][Tf_2N]	1-hexanol	13800 ± 1400	−45 ± 4.0	36300 ± 4800	−64 ± 13.5	1.08
[bmim][Tf_2N]	1-butanol	−42 ± 1800	−14 ± 6.1	59700 ± 3300	−160 ± 11.3	0.26
[bmim][Tf_2N]	1-hexanol	11800 ± 1900	−44 ± 6.0	29500 ± 4500	−55 ± 14.0	0.68
[hmim][Tf_2N]	1-hexanol	23000 ± 1100	−89 ± 3.7	27400 ± 2000	−48 ± 6.6	0.35
[hmim][Tf_2N]	1-octanol	21400 ± 1100	−76 ± 3.3	26700 ± 3800	−41 ± 11.7	0.36
[hmmim][Tf_2N]	1-hexanol	28100 ± 1100	−100 ± 3.4	16300 ± 1200	−5.0 ± 3.7	0.53
[omim][Tf_2N]	1-octanol	28300 ± 1300	−106 ± 3.9	21300 ± 400	−26 ± 1.1	0.25
[bmpy][Tf_2N]	1-butanol	29000 ± 2100	−113 ± 6.9	3700 ± 2100	34 ± 7.2	0.12
[bmpy][Tf_2N]	1-hexanol	21400 ± 300	−77 ± 1.1	20800 ± 1800	−21 ± 5.7	0.34
[hpy][Tf_2N]	1-hexanol	22600 ± 1600	−87 ± 5.2	26900 ± 600	−45 ± 2.1	0.18
[hmpy][Tf_2N]	1-hexanol	21700 ± 1800	−85 ± 6.0	23100 ± 400	−32 ± 1.3	0.21
[hmpy][Tf_2N]	1-hexanol	21300 ± 1200	−84 ± 3.9	18200 ± 1600	−13 ± 5.3	0.26
[hmDMApy][Tf_2N]	1-hexanol	24000 ± 800	−93 ± 2.7	12300 ± 400	8.5 ± 1.1	0.28
[hemmpy][Tf_2N]	1-hexanol	23900 ± 600	−92 ± 2.1	12600 ± 400	8.3 ± 1.2	0.41
[bmim][TfO]	1-dodecanol	30600 ± 2500	−85 ± 7.7	79500 ± 1200	−230 ± 3.9	0.85

differences between the computed (*c*) and experimental (*e*) values in both phases

$$\sigma = \left(\sum_i \left(\frac{x_{c,i}^{\mathrm{I}} - x_{e,i}^{\mathrm{I}}}{x_{e,i}^{\mathrm{I}}} \right)^2 + \left(\frac{x_{c,i}^{\mathrm{II}} - x_{e,i}^{\mathrm{II}}}{x_{e,i}^{\mathrm{II}}} \right)^2 \right)^{1/2} \quad (5)$$

and describes how well the linear dependent adjustable parameters reproduce the experimental data (i.e., the smaller the number, the better the fit). Both methods described here were used to correlate the experimental data. For all systems, the nonrandomness factor, α, was held constant at a value of 0.2.

A comparison of these two approaches is shown for the ionic liquid [bmpy][Tf_2N] with 1-hexanol in Figure 13 for the temperature-independent adjustable parameters and in Figure 14 for adjustable parameters with linear temperature dependence.

The modeled cloud point curve using the linear temperature-dependent parameters reproduced the experimentally observed data very well (Figure 14). In contrast, the temperature-independent adjustable parameters do not capture the curvature and asymmetry of the phase envelope, resulting in a poor fit of the experimental data (Figure 13). The results shown in Figures 13 and 14 are typical of the NRTL modeling of all of the systems investigated here, as well as all the IL/alcohol systems that we have studied in our previous work.[2,5] The adjustable parameters with linear temperature dependence were vastly better in reproducing the experimental phase equilibrium data than temperature-independent parameters. Overall, the binary interaction parameters with linear temperature dependence provided very good correlation of all of the experimental data.

Table 2 shows the linear fit information for the adjustable parameters, a_{ij} and b_{ij}, for all IL/alcohol systems presented here

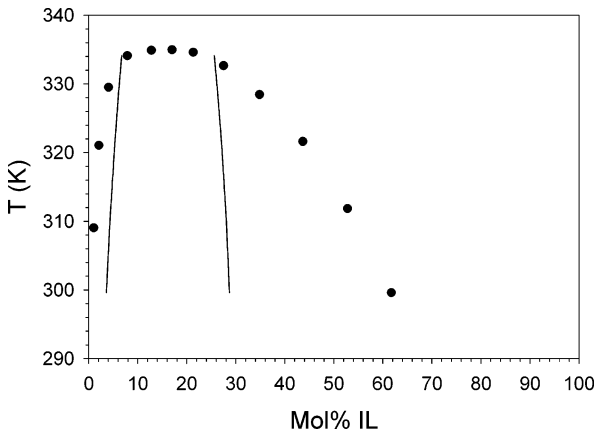

Figure 13. $T-x$ diagram for [bmpy][Tf_2N] (●) with 1-hexanol, with the predicted phase curve (—) using the NRTL equation with temperature-independent adjustable parameters.

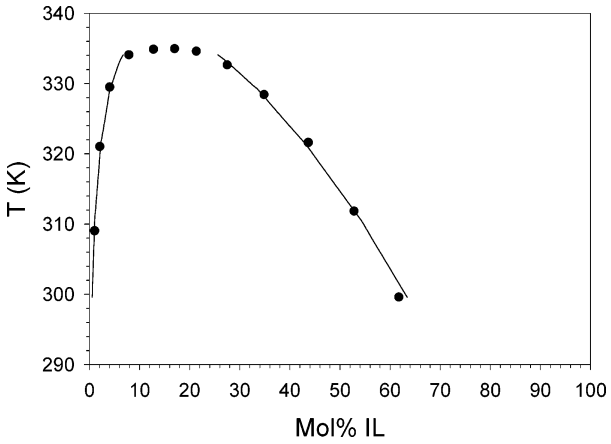

Figure 14. $T-x$ diagram for [bmpy][Tf_2N] (●) with 1-hexanol, with the predicted phase curve (—) using the NRTL equation with linear temperature-dependent adjustable parameters.

and in our previous publications.[2,5] Note that in our previous work we presented only the experimental data, without any NRTL modeling. Please see the previous publications for definitions of the IL abbreviations. In general, values of Δg_{12} are negative, typically between −2 and −6 kJ/mol, while values of Δg_{21} are positive, typically between 12 and 16 kJ/mol. This is exactly what we would expect on the basis of anticipated interaction energy between the species. Δg_{12} is the IL/alcohol interaction energy minus the alcohol/alcohol interaction energy. We would expect the IL/alcohol interaction to be stronger than the alcohol/alcohol interaction. Since all of these interactions are attractive and attractions have negative interaction energies, we would expect Δg_{12} to be negative. This is what we observe. By contrast, Δg_{21} is the IL/alcohol interaction minus the IL/IL interaction. Since we expect the IL/IL interaction to be very strong (due to Coulombic forces), this means we would anticipate large positive values for Δg_{21}. This is exactly what we observe. Additionally, the temperature dependence for Δg_{12} is greater than that for Δg_{21} in nearly all cases. This observation is consistent with the shape of the cloud point curves for all systems, with a larger temperature dependence for the alcohol solubility in the IL-rich phase than for the IL solubility in the alcohol-rich phase. Finally, the magnitude of Δg_{12} and Δg_{21} is quite reasonable. With the energy for a van der Waals interaction at 2−6 kJ/mol and a hydrogen bond at approximately 44 kJ/mol, the values for the adjustable parameters are consistent with two types of intermolecular interactions that are expected for IL/alcohol systems.

Conclusions

Knowledge of the impact of different factors on the liquid-phase behavior of ionic liquids with other liquids is useful for developing ionic liquids as "designer solvents" for specific applications. From this work, we have shown how the liquid−liquid phase behavior of pyridinium ionic liquids with alcohols is influenced by the characteristics of the IL and that similar behavior is observed for pyridinium and imidazolium ILs for corresponding features of the IL. An increase in the alkyl chain length of the alcohol results in an increase in the UCST, since the alcohol becomes more aliphatic and less able to interact with the IL through hydrogen bonding and dipolar and Coulombic forces. An increase in the length of one of the alkyl chains on the cation resulted in a decrease in the UCST, likely due to greater van der Waals interactions between the alkyl chain on the cation and the chain of the alcohol. The effect of anion on the UCST was observed to be related to the ability of the anion to accept a hydrogen bond, with [Tf_2N] ILs having a higher IL−alcohol mutual solubility than analogous [BF_4] ILs. The addition of methyl groups to a pyridinium cation had little impact on the phase behavior, while the addition of a dimethylamino group increased the UCST of the phase envelope slightly. The presence of an alkyl group at the C2 position of a pyridinium cation caused a significant increase in the UCST of the phase envelope, since this alkyl group may provide an impediment between the alkyl portion of the cation and the alkyl chain on the alcohol. However, the effect of C2 substitution for pyridinium ILs is less than that for imidazolium ILs, presumable due to the type of interactions involved, steric hindrance, and van der Waals interactions for pyridinium ILs versus hydrogen bonding for imidazolium ILs. Last, the strength of the cation−anion interaction will be a major determining factor in how the cation influences the liquid-phase behavior of these systems. All systems were modeled using the NRTL equation, with linear temperature-dependent adjustable parameters providing an excellent fit of the experimental data.

Acknowledgment. We acknowledge partial financial support for the project from the State of Indiana 21st Century Research and Technology Fund (909010455), the National Science Foundation (CTS-9987627), and the Department of Education (P200A010448-01). We also acknowledge the generous contribution from Reilly Industries of pyridine starting materials used in the synthesis of ILs for this work.

Supporting Information Available: Tables of liquid−liquid equilibrium data. This material is available free of charge via the Internet at http://pubs.acs.org.

References and Notes

(1) Anthony, J. L.; Anderson, J. L.; Maginn, E. J.; Brennecke, J. F. *J. Phys. Chem. B* **2005**, *109*, 6366−6374.
(2) Crosthwaite, J. M.; Aki, S. N. V. K.; Maginn, E. J.; Brennecke, J. F. *J. Phys. Chem. B* **2004**, *108*, 5113−5119.
(3) Fredlake, C. P.; Crosthwaite, J. M.; Hert, D. G.; Aki, S. N. V. K.; Brennecke, J. F. *J. Chem. Eng. Data* **2004**, *49*, 954−964.
(4) Crosthwaite, J. M.; Muldoon, M. J.; Dixon, J. K.; Anderson, J. L.; Brennecke, J. F. *J. Chem. Thermodyn.* **2005**, *37*, 559−568.
(5) Crosthwaite, J. M.; Aki, S. N. V. K.; Maginn, E. J.; Brennecke, J. F. *Fluid Phase Equilib.* **2005**, *228*−*229*, 303−309.
(6) Bonhote, P.; Dias, A. P.; Papageorgiou, N.; Kalyanasundaram, K.; Gratzel, M. *Inorg. Chem.* **1996**, *35*, 1168−1178.
(7) Cammarata, L.; Kazarian, S. G.; Salter, P. A.; Welton, T. *Phys. Chem. Chem. Phys.* **2001**, *3*, 5192−5200.
(8) Wu, C. T.; Marsh, K. N.; Deev, A. V.; Boxall, J. A. *J. Chem. Eng. Data* **2003**, *48*, 486-491.
(9) Heintz, A.; Lehmann, J. K.; Wertz, C. *J. Chem. Eng. Data* **2003**, *48*, 472−474.
(10) Domanska, U.; Marcinek, A. *J. Phys. Chem. B* **2004**, *108*, 2376−2382.
(11) Domanska, U.; Bogel-Lukasik, E.; Bogel-Lukasik, R. *J. Phys. Chem. B* **2003**, *107*, 1858−1863.
(12) Wagner, M.; Stanga, O.; Schroer, W. *Phys. Chem. Chem. Phys.* **2003**, *5*, 3943−3950.
(13) Crowhurst, L.; Mawdsley, P. R.; Perez-Arlandis, J. M.; Salter, P. A.; Welton, T. *Phys. Chem. Chem. Phys.* **2003**, *5*, 2790−2794.
(14) Morrow, T. I. Development and Application of Molecular Dynamics Methods to the Study of Ionic Liquids. Ph.D. dissertation, University of Notre Dame, 2005.
(15) Cadena, C.; Anthony, J. L.; Shah, J. K.; Morrow, T. I.; Brennecke, J. F.; Maginn, E. J. *J. Am. Chem. Soc.* **2004**, *126*, 5300−5308.
(16) Renon, H.; Prausnitz, J. M. *AIChE J.* **1968**, *14*, 135−144.
(17) Lin, Y.; Simoni, L. D.; Brennecke, J. F.; Stadtherr, M. A. In preparation.
(18) Heidemann, R. A.; Mandhane, J. M. *Chem. Eng. Sci.* **1973**, *28*, 1213−1221.